

# An investigation of the hidden structure of states in a mean field spin glass model.

Andrea Cavagna, Irene Giardina and Giorgio Parisi

*Dipartimento di Fisica, Università di Roma I 'La Sapienza', P.le A. Moro 5, 00185 Roma, Italy  
INFN Sezione di Roma I, Roma, Italy*

*cavagna@roma1.infn.it*

*giardina@roma1.infn.it*

*parisi@roma1.infn.it*

June 1997

## **Abstract.**

We study the geometrical structure of the states in the low temperature phase of a mean field model for generalized spin glasses, the  $p$ -spin spherical model. This structure cannot be revealed by the standard methods, mainly due to the presence of an exponentially high number of states, each one having a vanishing weight in the thermodynamic limit. Performing a purely entropic computation, based on the TAP equations for this model, we define a constrained complexity which gives the overlap distribution of the states. We find that this distribution is continuous, non-random and highly dependent on the energy range of the considered states. Furthermore, we show which is the geometrical shape of the threshold landscape, giving some insight into the role played by threshold states in the dynamical behaviour of the system.

PACS number: 75.10.N, 05.20, 64.60.c

## 1. Introduction.

Despite some recent developments [1,2,3], a deep understanding of the structure of the states in the  $p$ -spin spherical model is still lacking. The problem is the following:

In the context of the TAP approach [4], it has been shown that, in the temperature range between the static and the dynamical transition, this model has an exponentially high number of states (TAP solutions), with free energy densities in a finite range  $[f_{min}, f_{th}]$ . What happens is that *equilibrium* states at temperature  $T$  are not the lowest ones corresponding to  $f_{min}$ , but rather those which optimize the balance between the free energy and the entropic contribution due to the presence of a great number of states with the same free energy. Thus equilibrium states are those which minimize the generalized free energy density  $\phi(f) = f - T\Sigma(f)$ , where  $\Sigma$  is the *complexity*. The states with free energy density  $f$  either lower or larger than the value which minimizes  $\phi$  must be considered as metastable. On the other hand, *all* these states, the equilibrium as well as the metastable ones, singularly taken have a vanishing weight in the thermodynamic limit. In this sense, an equilibrium state is not different from a metastable state, since the equilibrium condition is a fully collective effect [1,5].

It is clear that the presence of this huge number of states makes it interesting to know how they are disposed in the phase space, and therefore to investigate their distribution and structure.

To clarify what we intend with structure of the states it is useful to think about the Sherrington-Kirkpatrick (SK) model [6]. In this case, in the context of the replica method, the solution given in [7,8,9] has permitted to define and calculate the overlap distribution  $P(q)$  of the pure states:  $P(q)$  is defined as the probability that, picked up two states, their mutual overlap is equal to  $q$ . Therefore, in the distribution  $P(q)$  two different contributions are present: the existence of states having mutual overlap  $q$  and their individual statistical weights. The function  $P(q)$  gives for the SK model an important structural information on the distribution of the states in term of the overlap [10].

For the  $p$ -spin spherical model we would like to have a structural information of the same kind as the one given by the distribution  $P(q)$  for the SK model.

Unfortunately, it is known that applying the standard replica method to the  $p$ -spin spherical model a trivial result is obtained [11]: in the intermediate temperature phase that we are considering, the model is solved by a replica symmetric solution, corresponding to a trivial distribution function  $P(q) = \delta(q)$ . This delta function simply means that the *typical* overlap between two states is zero. On the other hand, one can wonder why this distribution does not get contribution from the self overlap of the equilibrium states, which is different from zero. The answer is that all these states have singularly a weight so low that the contribution of their self overlap is not present in the distribution  $P(q)$ . In other words, it is highly unlikely to pick up twice the same state and measure its self overlap, either if this is an equilibrium state or a metastable one.

For the same reason it is possible that the distribution  $P(q)$  does not catch a contribution from *all* the other possible values of the overlap  $q$ , simply because picking up two states with overlap different from zero has a vanishing probability in the thermodynamic limit. This would mean that the trivial form of  $P(q)$  is not a consequence of the absence of states with mutual overlap different from zero, but rather of the difficulty of finding them [12]. On the contrary, there is the possibility that indeed *all* the states of this model have mutual overlap zero, i.e. that states with overlap different from zero do not exist at all. In this last case it is clear that there would be only a trivial structure of the states, exactly reproduced by a trivial  $P(q)$ . The standard static approaches cannot distinguish between these two pictures, and more than this, in the case in which a non trivial hidden structure were present, they are not able to give us

any insight into the problem. In our opinion it seemed very strange to have this huge number of states without any interesting geometrical structure and therefore we have tried to develop some non standard methods which could provide some information on this topic.

The first question to answer is then if a non trivial structure of the states, worth being investigated, exists. This question has been partially answered in the context of the real replica method, by the definition of a three replica potential [3]. Within this method it has been possible to demonstrate that, given an equilibrium state, there are other states, both metastable and equilibrium, at *any* value of the overlap  $q$  with it, until a certain maximum value. This shows clearly that a non trivial structure of the states for this model is present, and that the second picture we have stated above has to be discarded. On the other hand, the shape of the energy spectrum of the states found with this method was not completely understood and besides there was no control on the choosing procedure of the detected states.

Therefore it is necessary to define a tool by which the hidden structure of the states for the  $p$ -spin spherical model can be analyzed in a deep way. Yet, as we have seen, there is the problem of the vanishing weight of these states, that leads to the trivial form of the standard distribution function  $P(q)$ .

Bearing this in mind, the most natural thing to do is to perform a purely entropic computation, disregarding the thermodynamic weight of the states. Thus, what we have done is to fix a reference state in the phase space and simply *count* how many states of a given kind are present at overlap  $q$  with it. More precisely, what we have actually computed is the number of TAP solutions having a given overlap  $q$  with a single fixed solution. The resulting quantity is what we have called the *constrained complexity*  $\Sigma_c$ .

To conclude this Introduction we want to stress a point that could seem trivial, but that has some importance in our opinion. We said that we wanted to study the structure of the *states* of this model, but actually we work with *solutions* of the TAP equations. The underlying hypothesis is then that TAP solutions really correspond to thermodynamic states, intended as local minima of the *true* free energy of the system. This is not a trivial identification, but it has been confirmed in various ways [2,13,3]. For example, in the case of the three replica potential of [3], one can show that the local minima of the potential, which correspond to metastable states of the system, always have a free energy and a self overlap that satisfy TAP equations.

The Paper is organized in the following way: In Section 2 we define the constrained complexity and describe the way in which the calculation has been performed. The main results are exposed in Section 3, where the behaviour of  $\Sigma_c$  is analyzed and interpreted in terms of geometrical structure of the states. In Section 4 we address the question of which are the dominant states at a certain distance from a reference equilibrium state, while in Section 5 we focus on the structure of the threshold states, which are important under many respects. In Section 6 we state the conclusions and outline the most important open problems. Finally, the comparison with the results of the real replica method is carried out in a detailed way in Appendix A.

## 2. The constrained complexity.

The  $p$ -spin spherical model is defined by the following Hamiltonian

$$H(s) = - \sum_{i_1 < \dots < i_p} J_{i_1 \dots i_p} s_{i_1} \dots s_{i_p} \quad (2.1)$$

where the spins  $s$  are real variables satisfying the spherical constraint  $\sum_i s_i^2 = N$  ( $N$  is the size of the system) and the couplings  $J$  are Gaussian variables with zero mean and variance  $p!/2N^{p-1}$  [14,15,11].

In the frame of the TAP approach [4], one formulates mean field equations for the local magnetizations  $m_i = \langle s_i \rangle$  of the system. In [1] it has been introduced a free energy density  $f_{TAP}$ , function of the magnetizations  $m_i$ , minimizing which one obtains the TAP equations of the system. Solving these equations at  $T = 0$  one finds minima of  $f_{TAP}$  with energy density included in a finite range  $[E_{min}, E_{th}]$ . The solutions with the highest energy density  $E_{th}$  are usually called *threshold* solutions. For each value of the energy density  $E$  in this range, there is an exponentially high number of solutions

$$\mathcal{N}(E) \sim e^{N\Sigma(E)} \quad (2.2)$$

where  $\Sigma(E)$  is the *complexity* of the class of TAP solutions corresponding to that particular energy. The complexity  $\Sigma(E)$  for this model has been computed in [5], where it is found that  $\Sigma$  is an increasing function of  $E$ , which is zero for  $E = E_{min}$  and reaches a finite value for  $E = E_{th}$ . Moreover, due to the particular homogeneity of the Hamiltonian, there is a one to one mapping of the solutions found at temperature zero, into solutions at finite temperature  $T$ , without splitting nor merging of solutions with varying the temperature. Due to this, one can solve TAP equations at  $T = 0$ , obtaining a class of solutions with a certain zero temperature energy density  $E$  and then transport these solutions to finite  $T$ . Therefore from now on we will identify a TAP solution with its zero temperature energy density  $E$ , even if we are considering this solution at finite temperature  $T$ . The important thing is that the complexity  $\Sigma(E)$  of a given class does not depend on  $T$ , but only on the zero temperature energy  $E$  of this class, while the self overlap of each solution depends both on  $E$  and on the temperature  $T$ .

We now introduce the constrained complexity:

$$\Sigma_c(E_2, q|E_1) \stackrel{\text{def}}{=} \lim_{N \rightarrow \infty} \frac{1}{N} \overline{\log \mathcal{N}(E_2, q|E_1)}. \quad (2.3)$$

In this definition  $\mathcal{N}(E_2|q, E_1)$  is the number of TAP solutions with energy density  $E_2$  having overlap  $q$  with a single fixed solution of energy density  $E_1$ . The bar indicates the average over the disorder. What we are doing here is to fix a single state of energy  $E_1$  and simply count how many states of energy  $E_2$  are found at overlap (distance)  $q$  with it. We remark that  $q$  is the overlap between these TAP solutions at finite temperature, while  $E_1$  and  $E_2$  are their zero temperature energy densities.

In definition (2.3) we have averaged the logarithm of  $\mathcal{N}$ , since we expect that this is the extensive quantity. Therefore, to perform this average it is necessary to introduce replicas. However, it can be shown that in the unconstrained case [5], the correct ansatz for the overlap matrix is symmetric and diagonal and this is equivalent to average directly the number  $\mathcal{N}$  of the solutions. In our case the same prescription leads to the following definition:

$$\Sigma_c(E_2, q|E_1) \stackrel{\text{def}}{=} \lim_{N \rightarrow \infty} \frac{1}{N} \log \overline{\mathcal{N}(E_2, q|E_1)} \quad (2.4)$$

and this is the quantity we shall compute. It is surely possible that the introduction of the constraint  $q$  requires a breaking of the replica symmetry and therefore definition (2.4) has to be considered as a first approximation. Yet, as we shall show, the results obtained with formula (2.4) suggest that this is a good approximation.

The complexity  $\Sigma_c$  can be obtained by counting all pairs of solutions with energies  $(E_1, E_2)$  at mutual overlap  $q$  and dividing it by the number of solutions with energy  $E_1$ , i.e.

$$\Sigma_c(E_2, q|E_1) = \lim_{N \rightarrow \infty} \left\{ \frac{1}{N} \log \overline{\mathcal{N}(E_1, E_2, q)} - \frac{1}{N} \log \overline{\mathcal{N}(E_1)} \right\} \stackrel{\text{def}}{=} \Gamma(E_1, E_2, q) - \Sigma(E_1) \quad (2.5)$$

where  $\Sigma(E_1)$  is the usual unconstrained complexity computed in [5]. We note that the quantity  $\Gamma$  is symmetric in  $(E_1, E_2)$  while  $\Sigma_c$  is not. Moreover,  $\Gamma(E_1, E_2, 0) = \Sigma(E_1) + \Sigma(E_2)$ , since *almost* all TAP solutions are mutually orthogonal, and then

$$\Sigma_c(E_2, 0|E_1) = \Sigma(E_2) . \quad (2.6)$$

This is the first check we have to face in our calculation.

Let  $m_i^{(1)}$  and  $m_i^{(2)}$  be two solutions with self overlaps  $q_1$  and  $q_2$ , and mutual overlap  $q$ ; using the notation  $m \cdot m' = \sum_i m_i m'_i$ , we have

$$m^{(1)} \cdot m^{(1)} = Nq_1 \quad ; \quad m^{(2)} \cdot m^{(2)} = Nq_2 \quad ; \quad m^{(1)} \cdot m^{(2)} = Nq \quad (2.7)$$

Following [1] we write TAP equations in terms of the angular part of the magnetizations  $m_i$

$$\sigma_i = \frac{m_i^{(1)}}{\sqrt{q_1}} \quad ; \quad \tau_i = \frac{m_i^{(2)}}{\sqrt{q_2}} \quad (2.8)$$

for which it holds

$$\sigma \cdot \sigma = N \quad ; \quad \tau \cdot \tau = N \quad ; \quad \sigma \cdot \tau = N \frac{q}{\sqrt{q_1 q_2}} \stackrel{\text{def}}{=} Nq_0 . \quad (2.9)$$

In terms of the angular variables  $\sigma$  and  $\tau$ , the TAP equations read

$$0 = -p \sum_{i_2 < \dots < i_p} J_{i, i_2 \dots i_p} \sigma_{i_2} \dots \sigma_{i_p} - pE_1 \sigma_i \stackrel{\text{def}}{=} \mathcal{T}_i(\sigma; E_1) \quad , \quad i = 1, \dots, N \quad (2.10)$$

where  $E_1$  is the zero temperature energy density

$$E_1 = -\frac{1}{N} \sum_{i_1 < \dots < i_p} J_{i_1 \dots i_p} \sigma_{i_1} \dots \sigma_{i_p} . \quad (2.11)$$

Relations of the same kind of (2.10) and (2.11) hold for  $\tau$  and  $E_2$ . It is now possible to write  $\Gamma$  with the standard method of [16,5] in the following way:

$$\begin{aligned} \Gamma(E_1, E_2, q) &= \\ &= \frac{1}{N} \log \int \mathcal{D}P(J) \int \mathcal{D}\sigma \mathcal{D}\tau \prod_i \delta(\mathcal{T}_i(\sigma; E_1)) \delta(\mathcal{T}_i(\tau; E_2)) \left| \det \left( \frac{\partial \mathcal{T}(\sigma; E_1)}{\partial \sigma} \right) \right| \left| \det \left( \frac{\partial \mathcal{T}(\tau; E_2)}{\partial \tau} \right) \right| \times \\ &\times \delta(\sigma \cdot \sigma - N) \delta(\tau \cdot \tau - N) \delta(\sigma \cdot \tau - Nq_0) \end{aligned} \quad (2.12)$$

with

$$\mathcal{D}P(J) = \prod_{i_1 < \dots < i_p} \sqrt{\frac{N^{p-1}}{\pi p!}} \exp(-J_{i_1 \dots i_p}^2 N^{p-1}/p!) dJ_{i_1 \dots i_p} . \quad (2.13)$$

We note that the dependence on the temperature is entirely contained in  $q_0$  through  $q_1$  and  $q_2$ , functions respectively of  $E_1, E_2$  and  $\beta$  [1].

In formula (2.12) we can drop the two modulus since it is possible to check *a posteriori* that the determinants are positive. Actually, this is a tricky point. As shown in [17,18], if one counts the stationary points of a function neglecting the modulus in integrals of the kind (2.12), a trivial result is obtained, due to the Morse theorem. Nevertheless, we note that we are not calculating here the whole number of stationary points of the TAP free energy, but we are counting those *with a given energy density*.

Moreover, for energies lower than the threshold, the dominant contribution to the determinant is truly positive, as can be shown by computing the Hessian spectrum of the TAP free energy. On the other hand, the same procedure of removing the modulus gives the normal unconstrained TAP complexity of [5], which has been confirmed in [2] with a totally different method.

In order to perform the calculation it is useful to write both these determinants by means of a Fermionic representation

$$\det A = \int d\bar{\psi}d\psi e^{-\sum_{ij} \bar{\psi}_i A_{ij} \psi_j} \quad (2.14)$$

while the usual (Bosonic) integral representation is adopted for the delta functions which implement the TAP equations in (2.12). The average over the disorder  $J$  generates couplings among Bosonic and Fermionic variables, but these mixed couplings are set equal to zero as in the unconstrained calculation. In this way it is possible to average separately the Fermionic part from the Bosonic one. This simplifies a lot the calculation, since it turns out that the Fermionic part has exactly the same form as in the unconstrained case, while, due to the presence of the constraint  $q_0$ , this is no longer true for the Bosonic part. We can write the unconstrained complexity in the usual following way (see [5]):

$$\Sigma(E) = \Xi(E)_{Bosons} + \Omega(E)_{Fermions} \quad (2.15)$$

with

$$\Xi(E) = \frac{1}{2} \log(2/p) - \frac{1}{2} - E^2 \quad ; \quad \Omega(E) = -pEz - \frac{p(p-1)}{4} z^2 - \log z \quad (2.16)$$

$$z = \frac{-E - \sqrt{E^2 - 2(p-1)/p}}{(p-1)}. \quad (2.17)$$

Similarly, for what said above, we can write

$$\Gamma(E_1, E_2, q) = \Delta(E_1, E_2, q) + \Omega(E_1) + \Omega(E_2) \quad (2.18)$$

where  $\Delta$  is the Bosonic contribution to (2.12). In this way  $\Sigma_c$  has the form

$$\Sigma_c(E_2, q|E_1) = \Delta(E_1, E_2, q) - \Xi(E_1) + \Omega(E_2). \quad (2.19)$$

Besides the variables  $\sigma$  and  $\tau$  there are two more Bosonic fields coming from the integral representation of the delta functions, respectively  $\mu$  and  $\lambda$ . All these Bosons couple because of the average over the disorder  $J$ . To perform the saddle point approximation we introduce the following set of variational parameters:

$$\begin{aligned} Nx_1 &= \mu \cdot \mu \quad ; \quad Nx_2 = \lambda \cdot \lambda \quad ; \quad Nx_3 = \mu \cdot \lambda \\ Ny_1 &= \sigma \cdot \mu \quad ; \quad Ny_2 = \tau \cdot \lambda \quad ; \quad Ny_3 = \sigma \cdot \lambda \quad ; \quad Ny_4 = \tau \cdot \mu. \end{aligned} \quad (2.20)$$

We remind that  $\sigma \cdot \tau = Nq_0$ , while  $\sigma \cdot \sigma = \tau \cdot \tau = N$ . The explicit calculation gives

$$\begin{aligned} \Delta(E_1, E_2, q) &= \\ &= \text{Ext}_{x,y} \left\{ ipE_1y_1 + ipE_2y_2 - \frac{p(p-1)}{2} q_0^{p-2} y_3y_4 - \frac{p}{4}(x_1 + x_2) - \frac{p}{2} q_0^{p-1} x_3 \right. \\ &\quad \left. - \frac{p(p-1)}{4} (y_1^2 + y_2^2) + \frac{1}{2} \log \left( \frac{\Lambda}{1 - q_0^2} \right) \right\} \end{aligned} \quad (2.21)$$

with

$$\Lambda = [x_1(1 - q_0^2) - k_1][x_2(1 - q_0^2) - k_2] - [x_3(1 - q_0^2) - k_3]^2 \quad (2.22)$$

$$k_1 = y_1^2 - 2q_0y_1y_4 + y_4^2 \quad ; \quad k_2 = y_2^2 - 2q_0y_2y_3 + y_3^2 \quad ; \quad k_3 = y_1y_3 - q_0(y_1y_2 + y_3y_4) + y_2y_4 \quad (2.23)$$

and we remind that  $q_0 = q/\sqrt{q_1q_2}$ . The saddle point equations are easily solved numerically, while it is possible to check analytically that for  $q_0 = 0$  we have  $\Delta(E_1, E_2, 0) = \Xi(E_1) + \Xi(E_2)$  and then equation (2.6) is fulfilled.

### 3. Normal and anomalous regimes.

In this Section we analyze the dependence of the constrained complexity  $\Sigma_c$  on  $E_2$  and  $q$ , at a fixed value of  $E_1$ . In particular, we focus our attention on the dependence of  $\Sigma_c$  on the overlap  $q$ , since we are interested in the overlap spectrum of the system, this giving information on the geometrical distribution of the states in the phase space. In what follows it is always assumed  $T \in [T_s, T_d]$ , where  $T_s$  and  $T_d$  are respectively the static and the dynamical transition temperatures.

As a value for the reference energy  $E_1$  we choose  $E_1 = E_{eq}(\beta)$ , where  $E_{eq}(\beta)$  is the zero temperature energy density of those TAP solutions that dominate at temperature  $\beta$ ; in this way, we are fixing an equilibrium state and counting how many states of energy density  $E_2$  are present at distance  $q$  from it. We stress however that we could choose any other value for the reference energy  $E_1$ , obtaining qualitatively the same results.

It is useful to distinguish two different regimes: a *normal* regime, corresponding to values of  $E_2$  well below the threshold, in which geometrical considerations at least qualitatively apply, and an *anomalous* regime, characterized by values of  $E_2$  just below the threshold, which shows a rather peculiar behaviour of  $\Sigma_c$ .

- *The normal regime:*

The normal regime is defined by values of the energy  $E_2$  of the states we are counting well below the threshold energy  $E_{th}$ . Intuitively, we expect that  $\Sigma_c$  decreases with increasing  $q$ , since this corresponds to consider smaller and smaller portions of the phase space into which looking for TAP solutions. This is indeed what happens in the normal regime, as shown in Figure 1, where we have plotted  $\Sigma_c$  as a function of  $q$ .

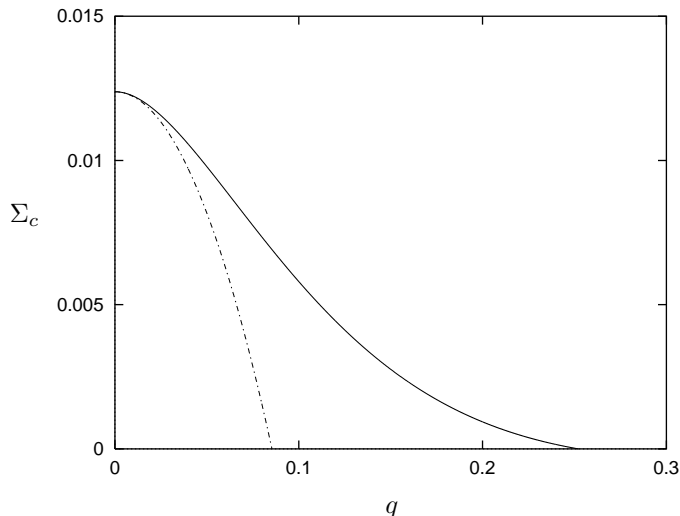


**Figure 1:** The constrained complexity  $\Sigma_c$  as a function of the overlap  $q$  (full line), with  $E_1=E_2=E_{eq}=-1.156$ , for  $\beta=1.64$  and  $p=3$ . The self overlap of the two states is  $q_1=q_2=0.55$ , while  $\Sigma_c=0$  at  $q_{last}=0.25$ . The dashed-dotted line is the curve predicted by a random distribution of the states (see the text). For  $q=0$  both the curves coincide with the unconstrained complexity  $\Sigma(E_2)$ .

This curve provides us some important information: First of all this is a *continuous* curve, meaning

that there is a continuous spectrum of states with energy  $E_2$  around the fixed reference state of energy  $E_1$  (in Figure 1 we have set  $E_2 = E_{eq}$ ). This means that there is an exponentially high number of states at any value of  $q$ , until a value  $q_{last}$  for which  $\Sigma_c = 0$ . Thus  $q_{last}$  gives the overlap of the nearest states with energy  $E_2$ . It is important that, as long as  $E_1$  and  $E_2$  are different from  $E_{th}$ , this value  $q_{last}$  is *smaller* than the self overlap of the considered states. This gap between the last value of the overlap in the spectrum and the self overlaps  $q_1, q_2$  simply means that these states are well separated one with respect to the other, i.e.

$$\frac{q_{last}}{\sqrt{q_1 q_2}} < 1 . \quad (3.1)$$

This has to be compared with the case of the Sherrington-Kirkpatrick model [6] in which as well as in this case there is a continuous distribution of states, but with mutual overlap going from  $q = 0$  up to the self overlap  $q = q_{EA}$  [10,19].

The second important feature of Figure 1 can be caught if we compare  $\Sigma_c$  with the corresponding quantity that would be obtained in the case of a *random* distribution of the states. The simplest hypothesis we can formulate on the geometrical structure of the states is that they are randomly distributed in the phase space: in this case, the number of states at distance  $q$  from a given fixed point in the phase space would be simply given by the total number of states multiplied by the volume of the manifold defined by fixing  $q$ , i.e.

$$\Sigma_{random} = \Sigma(E_2) + \frac{1}{2} \log \left( 1 - \frac{q^2}{q_1 q_2} \right) \quad (3.2)$$

where  $\Sigma(E_2)$  is the unconstrained complexity and  $q_1, q_2$  are the self overlaps of the two solutions. If we plot this quantity as a function of  $q$  and compare it with  $\Sigma_c(q)$  (Figure 1), it can be seen that there is a violation of the random distribution and that this violation goes in the direction of having an higher number of states when looking at small distances.

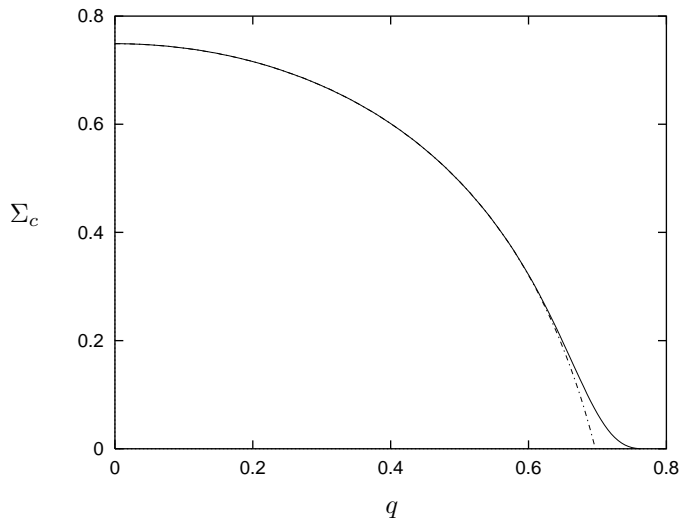


**Figure 2:** The constrained complexity  $\Sigma_c$  (full line), compared with the random distribution (3.2) (dashed-dotted line) for  $p=30$ . All other parameters are the same as in Figure 1.

The comparison with the random distribution of the states suggests an interesting check. It is known that the  $p$ -spin model in the limit  $p \rightarrow \infty$  coincides with the Random Energy Model of [20], which is characterized by a complete decorrelation of the energy levels of the system. Therefore we expect



that for increasing values of  $p$  the constrained complexity  $\Sigma_c$  gets more and more similar to the random distribution (3.2). This is shown in Figure 2, where we see that for  $p = 30$  it remains only a little tail for large  $q$  in which the two distributions are different. For  $p \rightarrow \infty$  they coincide. We note that in the Random Energy Model there is no geometrical structure at all. What we have here is that a complete *energetic* decorrelation between different states corresponds to a complete *geometrical* decorrelation in the phase space.

Finally we consider the dependence of  $\Sigma_c$  on the energy  $E_2$  of the states that we are counting. In Figure 3 we have plotted  $\Sigma_c(E_2)$  at various values of  $q$ . The curve on the top corresponds to  $q = 0$  and then reproduces the unconstrained complexity  $\Sigma(E_2)$  (see equation (2.6)). We note that, even at fixed  $q \neq 0$ ,  $\Sigma_c$  increases with increasing  $E_2$ , as in the unconstrained case. Furthermore, as expected, the whole curve  $\Sigma_c(E_2, q)$  decreases with increasing  $q$ .

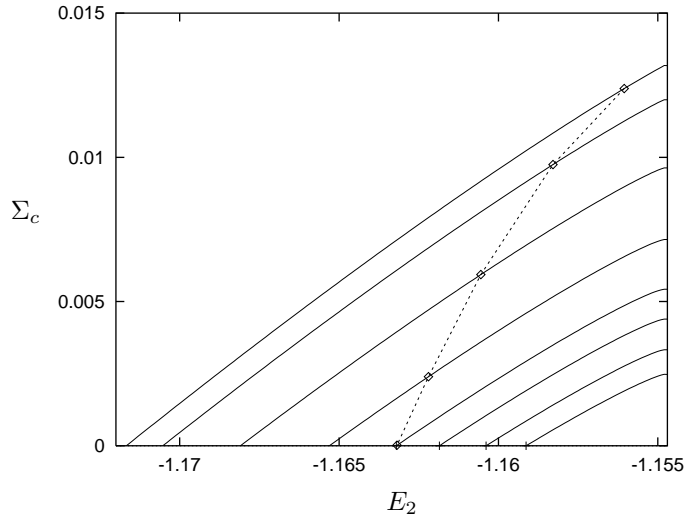


**Figure 3:** The constrained complexity  $\Sigma_c$  as a function of the energy  $E_2$ , at various values of the overlap  $q$  and  $E_1 = E_{eq} = -1.156$ , for  $\beta=1.64$  and  $p=3$ . The first curve on the top has  $q=0$  and thus corresponds to the unconstrained complexity  $\Sigma(E_2)$ . The threshold energy is  $E_{th} = -1.1547$ . The squares indicate the minimum of the function  $\phi_c$  (see Section 4), which reaches the axis  $\Sigma_c=0$  at  $q_{low}=0.113$ .

- *The anomalous regime:*

We turn now to examine the anomalous regime. If we plot  $\Sigma_c$  as a function of  $E_2$  exactly as in Figure 3, but now expanding a narrow range of energies  $E_2$  just below the threshold ( $E \in [E_{th} - 5 \times 10^{-4}, E_{th}]$ ), we obtain the behaviour shown in Figure 4.

The curves get lower and lower with increasing  $q$ , until for a value of  $q$  that we call  $q_{max}$  they begin to reverse, folding upwards. In Figure 4,  $q_{max}$  corresponds to the curve whose intersection with the  $\Sigma_c = 0$  axis starts going backward to the left with increasing  $q$ . If now we make a section of these curves at a fixed value of  $E_2$  in this range, plotting  $\Sigma_c$  as a function of  $q$ , we find the anomalous behaviour of Figure 5: there is an interval of  $q$  where  $\Sigma_c$  *increases* with increasing  $q$ .

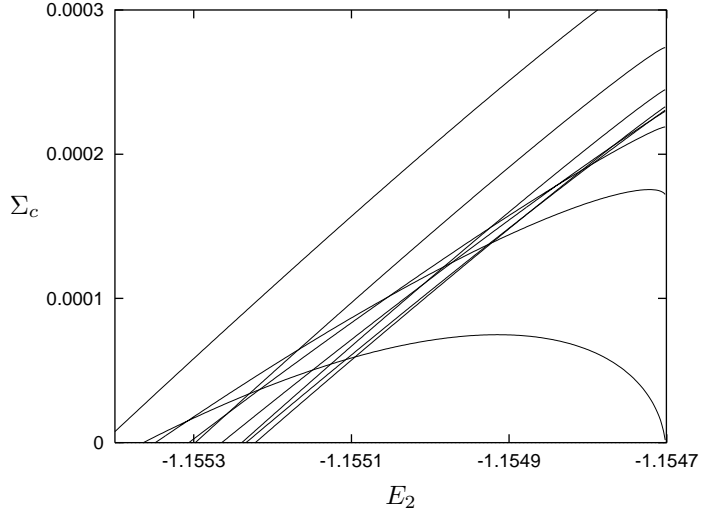


**Figure 4:** The constrained complexity  $\Sigma_c$  as a function of the energy  $E_2$  just below the threshold, at various values of  $q$ . The value  $q_{max}$  corresponds to the curve whose intersection with the axis  $\Sigma_c=0$  starts going to the left with increasing  $q$ .

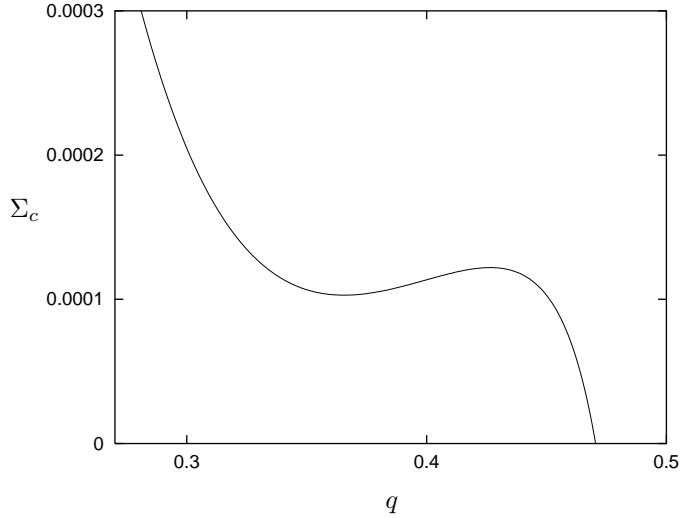


**Figure 5:** The constrained complexity  $\Sigma_c$  as a function of the overlap  $q$  in the anomalous regime.  $E_1=E_{eq}$  and  $E_2=-1.1550$ .

The reversed behaviour of  $\Sigma_c$  clearly has not a geometrical origin and for this reason we talk of an anomalous regime. What it seems is that, given a state (in this case an equilibrium state), there is a sort of clustering of states with high energy at small distances (large overlap) from it, thus giving the distribution of Figure 5. Moreover, from Figure 4 we note that for high enough values of  $q$ ,  $\Sigma_c$  is no longer monotonic with respect to  $E_2$ , and it develops a maximum. Therefore, in this range of  $q$  threshold solutions are no longer the most numerous around the fixed equilibrium state.

To conclude, we note that the amplitude of the anomalous regime depends on the reference energy  $E_1$ : the range of energies  $E_2$  into which this anomalous behaviour occurs is larger for low values of  $E_1$  and shrinks to zero as  $E_1$  approaches  $E_{th}$ .

#### 4. The spectrum of the dominant states.

At a first sight the increasing of  $\Sigma_c$  with  $q$ , together with the role of  $q_{max}$  in the anomalous regime could seem an artifact of the calculation. Nevertheless, how we are going to show, this behaviour is able to explain the energy spectra obtained with the real replica method of [3], where a completely different kind of computation is performed.

To face this problem we have to ask: Which are the *dominant* states at overlap  $q$  from a given fixed state? In the unconstrained case [1,5,13], equilibrium states of the system are defined as those TAP solutions that minimize the generalized free energy density  $\phi(f) = f - T\Sigma(f)$ . Similarly, we can wonder which solutions dominate at distance  $q$  from a given equilibrium state. To this end we look for the minimum of the function  $\phi_c(f, q) = f - T\Sigma_c(f, q)$ , with  $E_1 = E_{eq}$  and  $\Sigma_c$  expressed as a function of the free energy density  $f$  of the states found at distance  $q$ . In Figure 3, for each given value of  $q$ , we have signed on the corresponding curve the point that minimizes  $\phi_c$ . As it is easily seen, there is a value of  $q$  for which the minimum of  $\phi_c$  reaches the axis  $\Sigma_c = 0$ . We call this value  $q_{low}$ . If we look for a minimum of  $\phi_c$  when  $q > q_{low}$  we would be brought to a negative value of  $\Sigma_c$ , i.e. to non existing solutions (in the limit  $N \rightarrow \infty$ ). In this situation, the dominant solutions are those with the lowest energy density and a non negative value of the complexity, i.e. with  $\Sigma_c = 0$ . Due to this, at  $q_{low}$  there is a sharp change in the energy behaviour of the dominant solutions: this energy decreases following the minimum of  $\phi_c$  until  $q = q_{low}$ , then, for higher values of  $q$ , it increases following the intersection of the curves  $\Sigma_c(E_2)$  with the axis  $\Sigma_c = 0$ . Yet, from Figure 4 we see that when  $q$  reaches  $q_{max}$ , due to the anomalous behaviour of  $\Sigma_c$  this intersection point inverts its direction, and so the energy of the dominant solutions starts to decrease.

We conclude that the energy density of the solutions dominating at distance  $q$  from a fixed equilibrium state has a cuspid for  $q = q_{low}$  and reaches a maximum at  $q = q_{max}$ . What said above is shown in Figure 6.

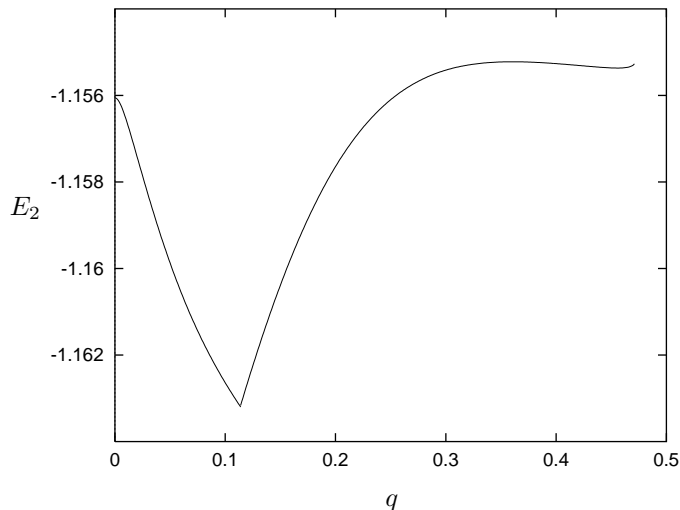


**Figure 6:** The energy density  $E_2$  of the solutions dominating at distance  $q$  from the fixed equilibrium solution. The cuspid is at  $q_{low}=0.113$  and the maximum is at  $q_{max}=0.360$ . The last point of the curve represents the distance of the nearest solutions.

In the real replica method usually a first replica is quenched into an equilibrium state, while a second

replica is forced to thermalize at distance  $q$  from it [2,3]. It is then natural to think that the second replica thermalizes into one of the states that dominate at distance  $q$  in the sense described above, and that therefore the spectrum of the states visited by this second replica is of the same kind as the spectrum of Figure 6. This is indeed what happens, as shown in more details in Appendix A: the spectrum found with the real replica method of [3] presents a cuspid, and has a maximum exactly at  $q = q_{max}$ , thus providing a confirmation of the existence of the anomalous regime.

In analyzing Figure 6 it is important to note that the number of dominant states is exponentially high in  $N$  as long as  $q < q_{low}$ , while it is of order  $N$  for  $q > q_{low}$ . In terms of constrained systems this transition is signaled by the breaking of the replica symmetry in the overlap matrix and this is another confirmation of the consistency of these two different methods (see Appendix A) [3,21].

The ending point of this curve corresponds to that value of the overlap above which no states of any energy are found with  $\Sigma_c \geq 0$ . Thus it indicates which is the overlap with the fixed state of energy  $E_1 = E_{eq}$  of the states nearest to it. It turns out that these nearest states have an energy density *greater* than the energy  $E_{eq}$  of the fixed reference state, even if in general they are not threshold states. What is important is that this is not a special feature of the equilibrium states: indeed, given a state of *any* energy  $E_1$ , the states nearest to it *always* have an energy density greater than  $E_1$ .

This behaviour is not a trivial consequence of the fact that states with higher energy are in general more numerous, since following this reasoning the nearest states would always be the threshold ones (which have the greatest unconstrained complexity), while we know that this is not true. Indeed, as mentioned in Section 3, at large values of the overlap  $q$ , i.e in the anomalous regime, threshold states are no longer the most numerous around a given fixed state. Once the curve of the dominant states of Figure 6 develops a maximum at  $q_{max}$ , it is not obvious which should be the energy of the states corresponding to the ending point of this curve.

## 5. The threshold states.

We turn now to examine the structure of the threshold states. We remind that threshold states are those solutions of the TAP equations with the highest energy density  $E_{th}$ . These states have a great importance under several aspects.

From a static point of view it can be shown that threshold states are *marginal*: the typical spectrum of the free energy Hessian evaluated in a TAP solution of energy  $E$  is a semicircle with support in the positive semi axis and its lowest eigenvalue  $\lambda_{min}$  goes to zero as  $E$  goes to  $E_{th}$ . In this sense threshold states develop some flat directions.

On the other hand, in the temperature range  $T < T_d$ , threshold states play a fundamental role in the off-equilibrium dynamics of this model. Solving analytically the dynamical equations with random initial conditions (i.e. high energy initial conditions), one finds that the asymptotic limit of the energy  $\mathcal{E}_\infty$  coincides with the threshold energy  $E_{th}$ . In other words, the asymptotic dynamics takes place at the threshold level, never visiting the sub threshold landscape. Moreover, the dynamical evolution of the system presents a first equilibrium regime in which the correlation function goes to the value of the self overlap of the threshold states  $q_{th}$ , followed by an off-equilibrium aging regime in which the correlation function goes to zero, this meaning that the system never truly thermalizes into any of the threshold states, but that rather it continuously drifts away [22].

Therefore it is intriguing to investigate the eventual relations between the peculiar dynamical behaviour that occurs at the threshold level and the geometrical structure of the threshold states.

To perform an analysis of this kind we set  $E_1 = E_2 = E_{th}$ , and we study the constrained complexity  $\Sigma_c$  as a function of  $q$ , i.e. we fix a threshold solution and count how many other threshold solutions are present at distance  $q$  from it. The corresponding curve is shown in Figure 7.

The important result is that

$$\Sigma_c(q) \rightarrow 0 \quad \text{for} \quad q \rightarrow q_{th}(\beta) \quad (5.1)$$

where  $q_{th}(\beta)$  is the self overlap of the threshold states at the temperature  $\beta$  we are considering. More precisely we find

$$\Sigma_c(q) \sim (q_{th} - q)^5 \quad \text{for} \quad q \sim q_{th} . \quad (5.2)$$

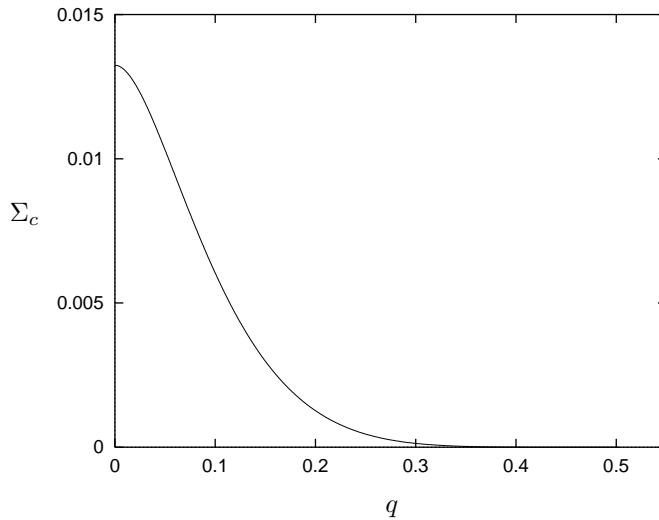


**Figure 7:** The constrained complexity  $\Sigma_c$  as a function of  $q$  with  $E_1=E_2=E_{th}$ , for  $\beta=1.64$  and  $p=3$ . For  $q>0.35$  the curve is indistinguishable from the axis and it reaches zero for  $q=q_{th}=0.504$ .

When the overlap between two states of the same kind is equal to their self overlap, it means that these two states are coincident in the thermodynamic limit. Thus, thinking of well separated states, one expects that  $\Sigma_c$  goes to zero at a value of  $q$  which is lower than the self overlap: indeed this is what happens for all the states below the threshold (see Figure 1 and equation (3.1)).

On the other hand, from (5.1) we see that, fixed a threshold state, other threshold states with vanishing complexity are found until a distance zero from the fixed one. A similar conclusion was deduced in [3], but in that context it was possible to state this result only at the dynamical transition temperature  $\beta = \beta_d$ , at which threshold states are the equilibrium ones. Here we see that this remains true at any temperature, as a natural consequence of the non chaoticity of TAP solutions with temperature.

As a consequence of equation (5.1) we can say that there is no sharp separation among threshold states, and that they rather form a structure of coalescent states. This means that these states are separated by free energy *density* barriers which are vanishing in the limit  $N \rightarrow \infty$ , i.e. that the free energy barriers grow as  $N^\alpha$  with  $\alpha < 1$  [23].

As previously said, these states are minima of the TAP free energy with some flat directions. We can then argue that they are connected along these flat directions, forming a sort of channel of states. Into this frame the dynamical drifting of the system (i.e. the decreasing to zero of the correlation function

in the off-equilibrium regime) can be viewed as a wandering along this channel of threshold states, in agreement with the ideas outlined in [22].

Finally, we note that, due to equation (5.1), the distribution of threshold states has no gap between the last value of the overlap in the spectrum and the self overlap, unlike all other sub threshold states. This feature is reminiscent of the overlap distribution in the Sherrington-Kirkpatrick model. Besides, we remind that in the SK model all the states are marginal, as it happens for the threshold states in the  $p$ -spin spherical model. From this point of view, we can say that threshold states are the most SK like.

## 6. Conclusions and open questions.

The  $p$ -spin spherical model for  $T_s < T < T_d$  is dominated by an exponentially high number of states, each one having a rather high free energy density  $f$  and therefore very small weight. This high free energy is counterbalanced by the entropic contribution of the complexity. Besides these equilibrium states, there is a great variety of metastable states, with free energy densities both lower and larger than the equilibrium one, all having a vanishing weight. In this sense, there is no real difference between equilibrium and metastable states, being the equilibrium a collective property.

In this situation, the standard replica approach fails, since it is not able to discriminate the overlap relations among all these states, while the TAP approach gives no information on the overlap distribution of them.

We have faced this problem introducing an overlap  $q$  between different TAP solutions and performing a purely entropic computation of their number. In this way we have defined a constrained complexity  $\Sigma_c(q)$ , which plays the role of the overlap distribution of the states.

By means of  $\Sigma_c$  we have found that the states are disposed in a non trivial way: fixed an arbitrary state from which observing the phase space, there is a continuous spectrum of states surrounding it. This means that there are states at each value of the overlap  $q$  with the reference one, from  $q = 0$  until a maximum value  $q_{last}$ . For sub threshold states there is a gap between this last value of the overlap and the value of the self overlap, meaning that they are well separated states. Moreover, the distribution is different from the one obtained supposing a random distribution of the states, since it shows a major crowding of states at small distances. Yet, the two distributions coincide in the  $p \rightarrow \infty$  limit, when the case of the Random Energy Model is recovered.

Furthermore, the analysis of threshold states has given some interesting results: these marginal states have an overlap distribution which goes continuously to zero at a value of  $q$  equal to their self overlap  $q_{th}$ . This means that these states are connected along their flat directions, forming a sort of channel that winds along the phase space. This feature may have a role in the asymptotic dynamics of the system, which occurs at the level of the threshold landscape.

To comment the continuous distribution of the overlap, and in particular the coalescent structure of the threshold states, we have often referred to the SK model, for which a continuous structure with respect to the overlap  $q$  is directly given by the standard distribution function  $P(q)$ . However, in doing this comparison it is necessary to make some specifications. In the ultrametric structure of the SK model the main role is played by the equilibrium states, which have the lowest free energy and finite weight, and whose number is of order  $N$ . This means that one can disregard the exponentially high number of states with higher free energy and vanishing weight (this can be done by introducing a cut-off on the branches

size of the ultrametric tree [24]). The situation for the  $p$ -spin spherical model is somehow the opposite: here the states, both of equilibrium and metastable, *all* have vanishing weight and are in exponentially high number. Therefore none of these states, whatever energy it has, can be disregarded. In this sense the investigation of the structure of the states for this model is complicated by the existence of a new relevant variable, that is the energy.

Moreover, we stress that there is at the present moment no evidence of an ultrametric organization of the states in the  $p$ -spin spherical model. To investigate this point it would be necessary to analyze the correlation among triplets of states, as it has been done for the SK model in [19]. The only fair indication of a clustering structure of the states comes from the existence of the anomalous regime, into which the constrained complexity grows with the overlap  $q$ . The existence of this anomalous regime is confirmed by the real replica method.

By means of the constrained complexity we have also obtained the spectrum of the dominant states at distance  $q$  from a given fixed state. This spectrum shows that below a certain value of the overlap, the number of the dominating states is exponential in  $N$ , while above this value (close states) this number is of order  $N$ . Besides, we have seen that the states nearest to any given state always have higher energy density.

We want to mention here a working hypothesis that could be useful for the present investigation. In the Generalized Random Energy Model of [25], an ultrametric structure is directly built in by defining the probability distributions of the energies at each clustering level. In this context, an equivalent of the functional order parameter  $x(q)$  of [7,8] can be identified. In [25] this construction is explicitly performed in the case of two clustering levels: in this simple example one can see that a function  $x(q)$  which *decreases* with increasing  $q$  corresponds to a hidden ultrametric structure, in the sense that this structure is present by construction, but is not revealed from the computation of the free energy of the system. This suggests that also for the  $p$ -spin spherical model, where a rich distribution of states is present but hard to reveal, an anomalous function  $x(q)$  could describe the underlying hidden structure. The existence of anomalous solutions of this kind in the context of the replica approach has been shown and discussed in [1,26,27,12].

To conclude, the main open issue on this topic is the pursuit of a unifying frame into which inserting all the results we have obtained, in order to describe in a synthetic way the rich and complex structure of states of the  $p$ -spin spherical model.

### **Acknowledgements.**

It is a pleasure to thank for important suggestions and very useful discussions Alain Barrat, Leticia Cugliandolo, Silvio Franz, Jorge Kurchan, Marc Mézard, Rémi Monasson, Heiko Rieger, Felix Ritort and Miguel Angel Virasoro.

## Appendix A: The comparison with the real replica method.

The real replica method [1,2,3,28] consists in studying the static properties of a certain number of real replicas of the system, as a function of the overlaps imposed among them. In [3] we introduced a three replica potential by which we analyzed the structure of equilibrium and metastable states of the  $p$ -spin spherical model: the first replica is fixed into an equilibrium state, while the second replica is forced to equilibrate at overlap  $q_{12}$  with the first one. Clearly, the way in which replica 2 chooses its constrained equilibrium state is heavily conditioned by the complexity  $\Sigma_c$  of the states at that distance. Once fixed replicas 1 and 2, the potential  $V_3$  is defined as the free energy density of a third replica 3 as a function of its distances  $q_{13}$  and  $q_{23}$  from the first two. The most important minimum of  $V_3$  corresponds to replica 3 in local equilibrium into the state chosen by replica 2. In this minimum, that we call  $M_2$ , the energy and the self overlap of replica 3 satisfy TAP equations, meaning that replicas 2 and 3 have found a state of the unconstrained system at distance  $q_{12}$  from the equilibrium state of replica 1.

Before proceeding further it is crucial to clarify the different roles of the three replicas, beginning from the way in which replica 2 chooses the state at distance  $q_{12}$  from 1. If the TAP free energy is minimized *on* the manifold defined by fixing  $q_{12}$ , the number of minima found is clearly greater than the number of *genuine* TAP solutions at that distance and for the most part consists of projections on the manifold of nearby true TAP solutions. These projections are what replica 2 sees as states. Therefore, we can say that replica 2 thermalizes in the vicinity of a TAP solution, but this solution is in general at distance  $q \neq q_{12}$  from replica 1. On the other hand, this TAP solution is that into which replica 3 thermalizes giving the minimum  $M_2$ , and this is why replica 3 gives the right TAP energy of this state and its right distance from replica 1, while replica 2 does not. To understand the energy spectrum of the states visited by replica 3, we must then investigate how replica 2 chooses these states.

As usual, replica 2 tries to optimize the balance between the free energy and the complexity of the solutions it finds on the manifold, minimizing a function  $\phi_2 = f_2 - T\Sigma_2(f_2, q_{12})$ . It is important to note that  $\Sigma_2$  is *not* the same function as  $\Sigma_c$ : There are *many* genuine TAP solutions with different TAP free energies  $f$  and at slightly different distances  $q$ , either higher or lower than  $q_{12}$ , whose projections on the manifold of replica 2 all have the same free energy  $f_2$ . Of these TAP solutions the relevant ones are those with the maximum complexity  $\Sigma_c(f, q)$ . This maximum value will then give  $\Sigma_2(f_2, q_{12})$ . Summarizing,  $\Sigma_2(f_2, q_{12})$  is equal to the complexity  $\Sigma_c$  of the most numerous TAP solutions whose projections on the manifold fixed by  $q_{12}$  have free energy  $f_2$  (the computation of  $\Sigma_2$  is explicitly performed in [21]).

The minimization of  $\phi_2$  with respect to  $f_2$  then selects a particular class of TAP solutions. Replica 2 is quenched into one of these solutions in the distorted way explained above, while replica 3 truly thermalizes into it. For this reason, the dependence on  $q_{12}$  of the energy of replica 3 in the minimum  $M_2$  is a mere manifestation of the process of equilibration of replica 2 above described.

Resuming, the states visited by replica 3 are chosen minimizing  $\phi_2$ , which does not coincide with the function  $\phi_c$  of Section 4 as well as  $\Sigma_2$  is not the same function as  $\Sigma_c$ . Nevertheless, it is clear that the spectrum given by the minimization of  $\phi_2$  must be similar to the one given by  $\phi_c$  in Section 4.

To make then a comparison with Figure 6, it is convenient to plot the zero temperature energy of replica 3 in the minimum  $M_2$  as a function of the overlap  $q_{13}$ , instead of  $q_{12}$ , since, as stated above,  $q_{13}$  better represents the real overlap between the two states. This parameterization is possible because in the minimum  $M_2$  the values of  $q_{13}$  is uniquely determined by  $q_{12}$ .



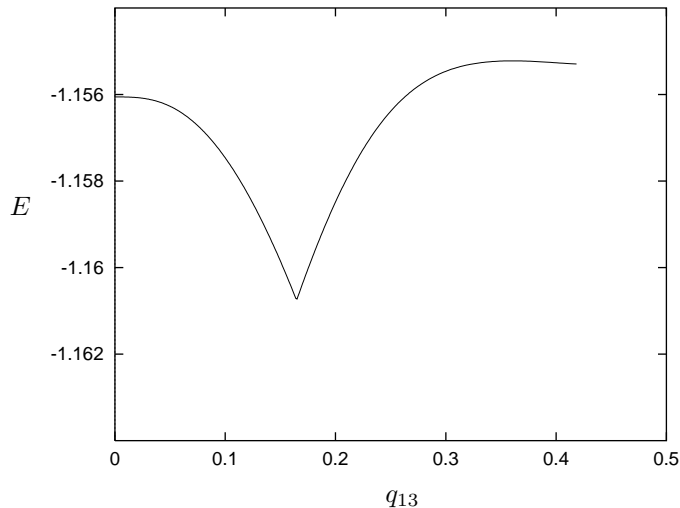


**Figure A1:** The energy density  $E$  of replica 3 in the minimum  $M_2$  of the three replica potential, as a function of the overlap  $q_{13}$ , for  $\beta=1.64$  and  $p=3$ . Here, as in Figure 6,  $q_{max}=0.360$ .

It can be seen from a comparison between Figure 6 and Figure A1 that, as we expected, the processes of minimization of  $\phi_c$  and  $\phi_2$  are qualitatively the same:

Firstly, we note from Figure A1 that there is a value of  $q_{13}$  for which the curve has a cusp; we call the corresponding value of  $q_{12}$  in the minimum  $M_2$  for which this cusp occurs,  $q_{rsb}$ . Indeed, following the same line of reasoning of Section 4, we argue that this cusp must correspond to the point in which  $\Sigma_2$  becomes zero. The computation developed in [3,21] shows that for value of  $q_{12}$  greater than  $q_{rsb}$  the overlap matrix  $Q^{22}$  of replica 2 breaks the replica symmetry. Physically, an RS form of the overlap matrix means either that the systems finds an exponentially high number of states (as in the  $p$ -spin model for  $T_s < T < T_d$ ), or that the phase space consists in just one state (as in the paramagnetic case). On the other hand, an RSB form means that the phase space is dominated by a number of order  $N$  of states (as in the  $p$ -spin model for  $T < T_s$ ). Therefore, the breaking of the replica symmetry of  $Q^{22}$  for  $q_{12} = q_{rsb}$  is a strong indication that here replica 2 ceases to see an exponentially high number of dominant states and confirms that in this point  $\Sigma_2$  becomes zero, as we argued above. As already stressed, the functions  $\phi_2$  and  $\phi_c$ , even though they have a similar physical meaning, are actually different and this is why the corresponding minimization curves (first branches in Figures 6 and A1) are different.

Secondly, in Figure A1 we note a maximum for  $q_{13} = q_{max}$ , i.e. exactly in the same point as in Figure 6. This is a consequence of the reversing in the behaviour of  $\Sigma_c$  that occurs in the anomalous regime. This behaviour is directly inherited by  $\Sigma_2$ : loosely speaking, if there are TAP solutions whose number starts to increase getting closer to the state of replica 1, the corresponding projections on a fixed manifold will increase too. This is an important confirmation of the role of the quantity  $q_{max}$  and, as a consequence, it is a confirmation of the existence of the anomalous regime.

Finally, it is worth observing that the ending points of the two curves are different, i.e. the potential  $V_3$  ceases to see states around replica 1 at a distance that is *greater* than the one corresponding to the nearest TAP solutions given by  $\Sigma_c$ . This can signify either that the potential fails to see these last states because replica 2 does not thermalizes in the vicinity of them, or that these last solutions given by  $\Sigma_c$  actually are not minima of the TAP free energy. At the present moment this is an open question.

Summarizing the considerations of this Appendix we can say that the energy spectrum given by the real replica method is well explained by the behaviour of the constrained complexity. This mutually confirms the results found with the two methods.

## References.

- [1] Kurchan J, Parisi G and Virasoro M A 1993 *J. Phys. I France* **3** 1819
- [2] Franz S and Parisi G 1995 *J. Phys. I France* **5** 1401
- [3] Cavagna A, Giardinà I and Parisi G 1996 cond-mat 9611068, to be published in *J. Phys. A: Math. Gen.*
- [4] Thouless D J, Anderson P W and Palmer R G 1977 *Philos. Mag.* **35** 593
- [5] Crisanti A and Sommers H-J 1995 *J. Phys. I France* **5** 805
- [6] Sherrington D and Kirkpatrick S 1975 *Phys. Rev. Lett.* **35** 1792
- [7] Parisi G 1979 *Phys. Rev. Lett.* **23** 1754
- [8] Parisi G 1980 *J. Phys. A: Math. Gen.* **13** L115
- [9] Parisi G 1980 *J. Phys. A: Math. Gen.* **13** 1887
- [10] Mézard M, Parisi G and Virasoro M A 1987 *Spin Glass Theory And Beyond*, World Scientific Publishing, Singapore
- [11] Crisanti A and Sommers H-J 1992 *Z. Phys. B* **87** 341
- [12] Virasoro M A 1996 *Simulated annealing methods under analytical control*, in B-L Hao (Ed), “Statphys 19” - Proc. of the 19th IUPAP Int’l Conf. on Stat. Phys., Xiamen, China, World Scientific Publishing, Singapore
- [13] Barrat A, Burioni R and Mézard M 1996 *J. Phys. A: Math. Gen* **29** L81
- [14] Gross D J and Mézard M 1984 *Nucl. Phys. B* **240** 431
- [15] Kirkpatrick T R and Thirumalai D 1987 *Phys. Rev. B* **36** 5388
- [16] Bray A J and Moore M A 1980 *J. Phys. C: Solid. St. Phys.* **13** L469
- [17] Vertechi D and Virasoro M A 1989 *J. Physique* **50** 2325
- [18] Kurchan J 1991 *J. Phys. A: Math. Gen* **24** 4969
- [19] Mézard M, Parisi G, Sourlas N, Toulouse G and Virasoro M A 1984 *J. Physique* **45** 843
- [20] Derrida B 1981 *Phys. Rev. B* **24** 2613
- [21] Barrat A, Franz S and Parisi G 1997 cond-mat 9703091
- [22] Cugliandolo L F and Kurchan J 1993 *Phys. Rev. Lett.* **71** 173
- [23] Kurchan J and Laloux L 1996 *J. Phys. A: Math. Gen* **29** 1929
- [24] Ruelle D 1987 *Commun. Math. Phys.* **108** 225
- [25] Derrida B 1985 *J. Physique* **46** L401
- [26] Ferrero M E 1993 Tesi di Laurea, Università degli Studi di Roma “La Sapienza”
- [27] Baviera R 1995 Tesi di Laurea, Università degli Studi di Roma “La Sapienza”
- [28] Franz S, Parisi G and Virasoro M A 1992 *J. Phys. I France* **2** 1869